

Pre-training Protein Models with Molecular Dynamics Simulations for Drug Binding

Fang Wu

Columbia University
New York, USA
fw2359@columbia.edu

Qiang Zhang *

Zhejiang University
Hangzhou, China
qiang.zhang.cs@zju.edu.cn

Dragomir Radev

Yale University
New Haven, USA
dragomir.radev@yale.edu

Yuyang Wang

Carnegie Mellon University
Pittsburgh, USA
yuyangw@cmu.edu

Xurui Jin

MindRank AI
Hangzhou, China
xurui@mindrank.ai

Yinghui Jiang

MindRank AI
Hangzhou, China
yinghui@mindrank.ai

Zhangming Niu *

MindRank AI
Hangzhou, China
zhangming@mindrank.ai

Stan Z. Li*

Westlake University
Hangzhou, China
stan.zq.li@westlake.edu.cn

Abstract

The latest biological findings discover that the motionless 'lock-and-key' theory is no longer applicable and the flexibility of both the receptor and ligand plays a significant role in helping understand the principles of the binding affinity prediction. Based on this mechanism, molecular dynamics (MD) simulations have been invented as a useful tool to investigate the dynamical properties of this molecular system. However, the computational expenditure prohibits the growth of reported protein trajectories. To address this insufficiency, we present a novel spatial-temporal pre-training protocol, PretrainMD, to grant the protein encoder the capacity to capture the time-dependent geometric mobility along MD trajectories. Specifically, we introduce two sorts of self-supervised learning tasks: an atom-level denoising generative task and a protein-level snapshot ordering task. We validate the effectiveness of PretrainMD through the PDBbind dataset for both linear-probing and fine-tuning. Extensive experiments show that our PretrainMD exceeds most state-of-the-art methods and achieves comparable performance. More importantly, through visualization we discover that the learned representations by pre-training on MD trajectories without any label from the downstream task follow similar patterns of the magnitude of binding affinities. This strongly aligns with the fact that the motion of the interactions of protein and ligand maintains the key information of their binding. Our work provides a promising perspective of self-supervised pre-training for protein representations with very fine temporal

*The corresponding authors.

resolutions and hopes to shed light on the further usage of MD simulations for the biomedical deep learning community.

1 Introductions

Drug discovery is an expensive process, where billions of dollars and years of development are required for a single drug to be approved by FDA [82]. To be specific, there are 10^{60} potential drug-like molecules, going far beyond current experimental capabilities [74]. Recently, deep learning (DL)-based methods have emerged to drastically reduce the molecular search space [5]. Drug binding, a core problem in drug discovery, is to understand how drug like molecules (ligands) interact with target proteins (receptors), and is a prerequisite for fast virtual screening [72, 87].

However, forecasting the strength of a candidate drug molecule’s interaction with a target protein brings unique challenges due to the evolution of binding theories. The initial ‘lock-and-key’ theory of ligand binding [25], where a frozen motionless receptor accommodates a small molecule without undergoing any conformational rearrangements, has been abandoned. It is now in favor of binding models that account not only for conformational changes, but also for random jiggling of receptors and ligands [85, 59, 10, 12, 91]. In other words, receptor and ligand flexibility are crucial for correctly predicting drug binding and related thermodynamic and kinetic properties [26, 1]. Notwithstanding, to the best of our knowledge, no preceding DL-based approaches take this sort of time-dependent mouldability into account. Instead, they typically consider a single, stable and static conformation for drug binding.

Motivated by above-mentioned reasons, we aim to explore the mechanism behind the binding recognition from not only a spatial but also a temporal perspective. While crystallographic studies convincingly demonstrate the important role that protein flexibility plays in drug binding, the expensive and extensive labor is demanded to generate them [22]. Alternatively, molecular dynamics (MD) simulations, first developed in the late 1970s [62], seek to overcome this limitation by using approximations based on Newtonian physics to simulation atomic motions, thus reducing the computational complexity [80]. This allows a thorough sampling of the conformational space, including that of large biomolecules, and can include, for example, the complete description of the pathway of the ligand binding to its target protein [17, 29, 77]. According to these facts, we employ MD to produce conformations of protein-ligand pairs in successive time-intervals.

Indeed, *ab initio* MD techniques have long and extensively been used to investigate structural and dynamical properties of a wide variety of molecular systems and understand the mechanism of physiochemical processes [89, 27, 88]. It substantially accelerates the studies to observe biomolecular process in action, particularly important functional processes such as ligand binding [79], ligand- or voltage-induced conformational change [19], protein folding [54], or membrane transport [52, 84].

The most basic and intuitive application of MD is to assess the mobility or flexibility of various regions of a biomolecule. Instead of yielding an average structure by experimental structure determination methods including X-ray crystallography and cryo-EM, MD allows researchers to quantify how much various regions of the molecule move at equilibrium and what types of structural fluctuations they undergo, which is critical for protein function and ligand binding [9, 44, 51]. To be explicit, on the one hand, simulations of the full ligand-binding process can reveal the binding site and pose of a ligand [21, 20, 43, 79]. On the other hand, at a quantitative level, simulation-based methods provide essentially more accurate estimates of ligand binding affinities (free energies) than other computational approaches such as docking [69].

Nevertheless, the high computational costs of MD still hinder the growing size of reported protein trajectories. Thus, a completely supervised paradigm of training and inference on MD trajectories of protein-ligand pairs seems infeasible. As a remedy, we resort to self-supervised learning (SSL) pre-training for the sake of empowering models with the ability to learn temporal dependencies. Recent studies have leveraged the large volume of unlabeled protein sequences to learn semantic representations [6, 7, 75, 24]. They take advantage of millions of sequences to pre-train protein encoders via SSL [18, 13, 96]. In addition, some methods [34, 98] start to directly capture the available protein structural information, which is proven to be the determinants of protein function. Despite the fruitful progress, none of prior work considers the exploitation of temporal sequences of protein structures.

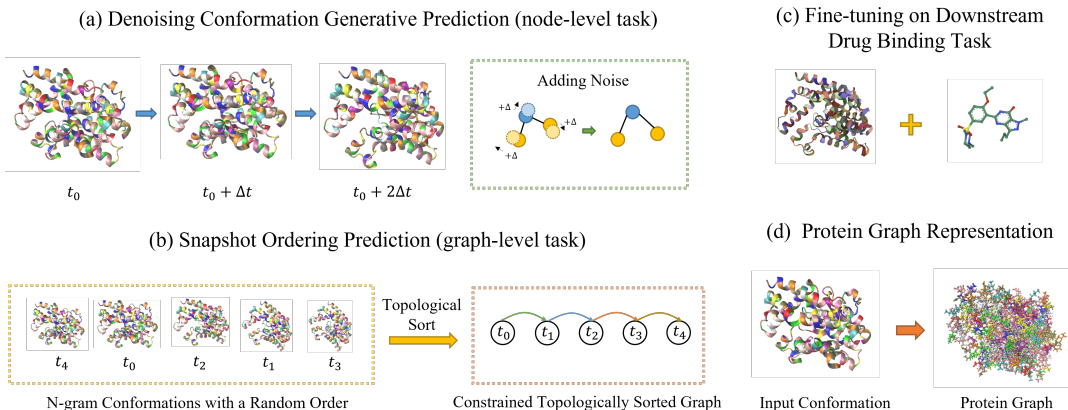


Figure 1: **Overview of our PretrainMD pipelines.** Sub-figures (a) and (b) portray the node-level and protein-level pre-training tasks. Sub-figure (c) illustrates the fine-tune of the pre-trained model in downstream protein-target binding affinity predictions. Sub-figure (d) delineates the graph representation of proteins to be fed as input for the protein encoder.

In this paper, we propose a simple yet effective pre-training framework with the full employment of MD trajectories called PretrainMD. It constructs two types of self-supervised tasks. The first is via the node-level denoising generative task. It increases the difficulty of the task by injecting additional noise into the input conformations, whose setting conforms to the principles of enhanced sampling mechanism in MD simulations [64]. The second is through the protein-level snapshot ordering task, which requires the model to recognize the temporal order of a set of consecutive snapshots. We pre-train a light Equivariant Graph Neural Network (EGNN) [78] with 0.05M parameters on the MD trajectories of 64 unlabeled protein-ligand pairs with 62.8K snapshots in total. The pre-trained geometric network is then leveraged for the downstream drug binding prediction task with both linear probing and fine-tuning. We test our model on the standard PDBbind dataset [93, 56]. Extensive experiments and visualizations demonstrate that models can learn effective representations with usage of abundant MD data, and pre-training can significantly and consistently improve the model performance.

2 Preliminary

Spatial-temporal protein sequences. We consider MD trajectories of each protein-ligand pair with T timesteps. $\mathcal{M}^{(t)} = (\mathbf{x}^{(t)}, \mathbf{h}^{(t)})$ denotes the conformation of both the protein and the small ligand at time $t \in [T]$ and is assumed to have N atoms. There $\mathbf{x}^{(t)} \in \mathbb{R}^{N \times 3}$ and $\mathbf{h}^{(t)} \in \mathbb{R}^{N \times \psi_h}$ denote the 3D coordinates and ψ_h -dimension roto-translational invariant features (e.g. atom types, electronegativity) associated with each atom, separately. We denote a vector norm by $x = \|\mathbf{x}\|_2$, and the relative position by $\mathbf{x}_{ij} = \mathbf{x}_i - \mathbf{x}_j$.

3 PretrainMD: Spatial-temporal Pre-training on MD Trajectories

Our model, termed as Pretraining on MD (PretrainMD), conducts SSL pre-training with simulated trajectories. The trajectories contain rich information about the energy and force changes along with the moving conformations, which are complementary to immobile conformations and play a key role in the determination of binding affinities. Since the success of the pre-training model crucially depends on the design of SSL tasks [76], we borrow ideas from the mature pre-training methods in the natural language process (NLP) field and introduce the following two assignments: a denoising conformation generative task and a snapshot ordering task (see Figure 1).

3.1 Denoising Generative Pre-training

Generative SSL is a classic track for unsupervised pre-training [47, 50, 46, 38]. It expects to learn effective representations by reconstructing each data point itself. Specifically to drug binding, a good SSL task should satisfy the following three essential properties: (i) the prediction target is reliable and easy to get. (ii) the prediction target should reflect the temporal information within the MD trajectories and relevant to the binding strength. (iii) learned presentations should be diverse and distinguishable. Guided by these criteria, we present the denoising generative prediction task. To be exact, we use the conformation of the next timeframe as the target and ask the model to forecast this prospective position. Given an unlabeled MD trajectory $\{\mathcal{M}^{(t)}\}_{t=1}^T$, we use a standard language modeling objective to maximize the following likelihood:

$$L_1 = \sum_{t=k+1}^T \log P\left(\mathbf{x}^{(t)} \mid \mathcal{M}^{(t-1)}, \dots, \mathcal{M}^{(t-k)}; \theta\right), \quad (1)$$

where k is the size of context window, and the conditional probability P is modeled via the protein encoder f_θ . Conventionally, several frameworks assume the Markov property on biomolecular conformational dynamics [14, 61] for ease of representation, i.e., $p\left(\mathbf{x}^{(t)} \mid \{\mathcal{M}^{(i)}\}_{i=0}^{t-1}\right) = p\left(\mathbf{x}^{(t)} \mid \mathcal{M}^{(t-1)}\right)$. We obey this rule and therefore set the length of context window as $k = 1$.

Moreover, we perturb the input conformation $\mathcal{M}^{(t-1)}$ with a little noise at each timestep. This operation of perturbation has both theoretical and empirical supports. As demonstrated by our latest work, the denoising diffusion architecture has a strong connectivity with the enhanced sampling method in MD [65], where energy is injected into the microscopic system to smooth biomolecular potential energy surface and decrease energy barriers. Besides, Godwin et al. [31] shows that the simple noise regularisation can be an effective way to address oversmoothing [11]. A noise correction target can be added to prevent oversmoothing by enforcing diversity in the last layers of our GNN, which is implemented with an auxiliary denoising autoencoder loss. In addition, we argue that as the difference between neighboring snapshots is small, the perturbation plays a critical part in preventing overfitting and improve generalization [2]. Towards this goal, the corrupted conformation is defined as $\tilde{\mathcal{M}}^{(t-1)} = \left(\tilde{\mathbf{x}}^{(t-1)}, \tilde{\mathbf{h}}^{(t-1)}\right)$, where $\tilde{\mathbf{x}}^{(t-1)} = \mathbf{x}^{(t-1)} + \sigma^{(t-1)}$ is constructed by adding a noise $\sigma^{(t-1)}$. The invariant atomic feature $\mathbf{h}^{(t-1)}$ can be either perturbed or not.

Note that random distortions of the geometry of proteins and molecules at a local energy minimum are almost certainly higher energy configurations [31]. This denoising procedure that maps from a noised molecule to a local energy minimum endows the model with eligibility to learn a map from high energy to low energy, which reveals the binding strength to some extent and maintains exactly the hidden information we expect to encode from MD trajectories.

3.2 Snapshot Ordering Pre-training

In order to train efficient conformation representations, we also refer to the classic sentence ranking task from NLP [39, 57], where the next sentence prediction (NSP) [18] is the most popular and basic one. In their setting, the model receives pairs of sentences as input and learns to predict if the second sentence is the subsequent one in the original document. It teaches the model to understand dependencies across sentences [53]. In spite of that, NSP is criticized as a weak task for its comparison of similarity [83]. To overcome this limitation, we introduce a harder snapshot ordering task, which aims to order a set of conformations as a coherent sub-trajectory. Specifically, a set of n conformations with the order $\mathbf{t} = \{t_i\}_{i=1}^n$ can be described as $\mathbf{M} = \{\mathcal{M}^{(t_i)}\}_{i=1}^n$. The goal is to find the correct order \mathbf{t}^* for them, i.e., $\mathbf{t}^* = [n]$, with which the whole sub-trajectory has the greatest coherence probability:

$$P\left(\mathbf{t}^* \mid \left\{\mathcal{M}^{(t_i)}\right\}_{i=1}^n\right) > P\left(\mathbf{t} \mid \left\{\mathcal{M}^{(t_i)}\right\}_{i=1}^n\right), \forall \mathbf{t} \in \psi, \quad (2)$$

where \mathbf{t} indicates any order of these conformations and ψ denotes the set of all possible orders. A series of approaches have been invented to tackle this rearranging problem [32, 58, 15, 94]. There we select the topological sort method [41, 70], a standard algorithm for linear ordering of the vertices of a directed graph. Precisely, we have \mathcal{C}_n set of constraints for this sub-trajectory. These constraints

\mathcal{C}_n represent the relative ordering between every pair of conformations in \mathbf{M} . Hence, we have $|\mathcal{C}_n| = \binom{v_i}{2}$, and constraints \mathcal{C}_n are learned using a multi-perceptron-layer (MLP) classifier. Notably, NSP is a special version of the snapshot ordering task if we make $n = 2$.

3.3 Protein Encoder

Equivariance is ubiquitous in deep learning for microscopic systems. This is because the physical law controlling the dynamics of atoms stays the same regardless of the rotation and translation of biomolecules [33]. Thus, it is essential to incorporate such inductive bias symmetry into model parameterization for modeling 3D geometry and achieving better generalization capacity [86, 48, 49, 78]. We draw inspirations from recent equivariant networks [86, 78] and employ a variant of EGNN as the protein encoder.

Specifically, the l -th layer of our encoder ($l \in [L]$) takes as input the set of atom embeddings $\mathbf{h}^{(t),l}$, and coordinates embeddings $\mathbf{x}^{(t),l}$. Then it outputs a transformation on $\mathbf{h}^{(t),l+1}$ and $\mathbf{x}^{(t),l+1}$. Concisely, $\mathbf{h}^{(t),l+1}, \mathbf{x}^{(t),l+1} = \text{Layer}(\mathbf{h}^{(t),l}, \mathbf{x}^{(t),l})$. We leave the details of the encoder in Appendix A.

After attaining the renewed atomic features, we use a simple global pooling [63] to aggregate the protein-level representations for the snapshot ordering task, as $\mathbf{H}^{(t)} = \text{Pool}\left(\left\{\mathbf{h}_i^{(t),L+1}\right\}_{i=1}^N\right) = \frac{1}{N} \sum_{i=1}^N \mathbf{h}_i^{(t),L+1}$.

3.4 Fine-tuning and Linear Probing

When fine-tuning, since there is only one snapshot for each protein-ligand pair, we omit the temporal superscript. Then we average pool \mathbf{h}_i across all atoms in both protein and ligand to extract a ψ_h -dimensional vector of features per example as $\mathbf{H} = \text{Pool}\left(\left\{\mathbf{h}_i\right\}_{i=1}^N\right)$. We aim to learn a projection from \mathbf{H} to binding affinities, which we use to minimize a root-mean-squared-error (RMSE) loss.

Extracting features for linear probing follows a similar procedure to fine-tuning, except that those features are fixed and the protein encoder does not participate in the backpropagation.

4 Experiments

To thoroughly evaluate the representations learned by our PretrainMD, we test its performance with both linear probing and fine-tuning, and compare it with multiple state-of-the-art methods on the benchmark drug binding dataset.

Dataset and Setup. We adopt the PDBbind database, a curated database containing protein-ligand complexes from the Protein Data Bank [8] and their corresponding binding strengths. The binding affinity provided by PDBbind is experimentally determined and expressed in molar units of the inhibition constant (K_i) or dissociation constant (K_d). Similar to prior work [67, 87, 81], we do not distinguish these constants and predict the negative log-transformed affinity as $pK = -\log(K)$. Besides, we select a 30% and a 60% sequence identity threshold to limit homologous ligands or proteins and split those complexes into training, test and validation.

As for the pretraining data collection, due to the limitation of computational resources, we choose 64 protein-ligand pairs in PDBbind and run MD simulations. Conformations of each protein-ligand pair at a series of time intervals are generated by OpenMM [23], a high-performance toolkit widely accepted for molecular simulation. In addition, we only use the pocket part instead of the whole protein for two major reasons. First, the pocket is the most critic region that the protein interacts with the ligand. Second, the pocket is much smaller and contains less atoms, so the training speed is significantly faster. To be specific, we locate the pocket as atoms in proteins whose minimum distance to the ligand is shorter than 10Å. More details regarding the experiments and conformation generations are elaborated in Appendix B

Baselines. We choose wide-ranging popular or state-of-the-art baselines for comparison. Among them, four methods are based on sequences including LSTM [6], TAPE [73], and ProtTrans [24].

Table 1: **Comparison of RMSD, R_p , and R_s on PDBbind.** The best performance is marked bold and the second best is underlined for clear comparison. Results are reported for 3 experimental runs.

Model	# Params	Pre.	Sequence Identity (30 %)			Sequence Identity (60 %)		
			RMSD	R_p	R_s	RMSD	R_p	R_s
Sequence-based Methods								
DeepDTA [67]	1.93M	No	1.565 ± 0.080	0.573 ± 0.022	0.574 ± 0.024	1.762 ± 0.261	0.666 ± 0.012	0.663 ± 0.015
LSTM [6]	48.8M	No	1.985 ± 0.016	0.165 ± 0.006	0.152 ± 0.024	1.891 ± 0.004	0.249 ± 0.006	0.275 ± 0.008
TAPE [73]	93M	No	1.890 ± 0.035	0.338 ± 0.044	0.286 ± 0.124	1.633 ± 0.016	0.568 ± 0.033	0.571 ± 0.021
ProtTrans [24]	2.4M	No	1.544 ± 0.015	0.438 ± 0.053	0.434 ± 0.058	1.641 ± 0.016	0.595 ± 0.014	0.588 ± 0.009
Surface-based Method								
MaSIF [28]	0.62M	No	1.484 ± 0.018	0.467 ± 0.020	0.455 ± 0.014	1.426 ± 0.017	0.709 ± 0.008	0.701 ± 0.011
Multi-scale Methods								
HoloProt [81]	1.44M	No	1.464 ± 0.006	0.509 ± 0.002	0.500 ± 0.005	1.365 ± 0.038	0.749 ± 0.014	0.742 ± 0.011
Structure-based Methods								
3DCNN [87]	2.1M	No	1.429 ± 0.042	0.541 ± 0.029	0.532 ± 0.033	1.450 ± 0.024	0.716 ± 0.008	0.714 ± 0.009
3DGCN [87]	0.37M	No	1.963 ± 0.120	0.581 ± 0.039	0.647 ± 0.071	1.493 ± 0.010	0.669 ± 0.013	0.691 ± 0.010
IEConv [35]	5.8M	No	1.554 ± 0.016	0.414 ± 0.053	0.428 ± 0.032	1.473 ± 0.024	0.667 ± 0.011	0.675 ± 0.019
PretrainMD (Linear-probing)	0.05M	Yes	1.417 ± 0.021	0.548 ± 0.036	0.564 ± 0.042	1.423 ± 0.014	0.665 ± 0.009	0.687 ± 0.011
PretrainMD (Fine-tuning)	0.05M	Yes	1.419 ± 0.027	0.551 ± 0.045	0.575 ± 0.033	1.468 ± 0.026	0.673 ± 0.015	0.691 ± 0.014

DeepDTA [67] takes in pairs of ligand and protein SMILES as the input. While, four approaches are established on molecular geometric structures. Molformer [95] is a variant of Transformer [90] and operates on 3D heterogeneous molecular graphs with motifs. IEConv [35] designs a convolution operator that considers the primary, secondary, and tertiary structure of proteins and a set of hierarchical pooling operators for multi-scale modeling. 3DCNN and 3DGCN [87] are also competitive 3D methods. Additionally, MaSIF [28] takes advantage of protein surfaces. HoloProt [81] introduces a multi-scale construction of protein representations, which connects surface to structure and sequence.

Results. Table 1 reports the root-mean-squared deviation (RMSD), the Pearson correlation (R_p), and the Spearman correlation (R_s) on PDBbind. Even though our backbone architecture EGNN has a extremely small model size with only 0.05M parameters, our PretrainMD still achieves comparable RMSD, Pearson and Spearman correlations to these state-of-the-art approaches.

It is worth noting that PretrainMD with linear-probing can realize a RMSE of 1.417 in the 30% sequence identity, better than all baselines. This indicates the strong capability and superiority of our pre-training method to learn efficacious representations for the estimation of drug binding. We further prove this claim via visualization (see Fig. 2). More importantly, our model is pre-trained only in the trajectories of 64 proteins, but examined in more than 3K proteins. This phenomenon strongly shows that our PretrainMD has great generalization. Thus, there seems no need to simulate the trajectories of a large number of protein-ligand pairs, and pre-training on a small group of binding pairs is adequate.

Besides, PretrainMD with linear probing commonly yields a lower RMSD, while PretrainMD with fine-tuning yields higher correlations. It can also be found that structured-based methods generally surpass sequence-based and surface-based approaches.

Visualizations and ablation studies. To intuitively observe the representations that our SSL tasks have learned, we envision the representations by mapping them to the two-dimensional space by TSNE algorithm [60]. (see Figure 2). Remarkably, even without any label information, the representations learned from SSL follow some kind of pattern that is strongly related to the magnitude of drug binding. This demonstrates that our designed SSL tasks are an appropriate way to excavate structural and dynamical properties of molecular systems and comprehend the mechanism of physiochemical processes within the MD trajectory.

We also conduct extensive experiments to exam the effects of each component in our PretrainMD with a 30% sequence identity threshold. First, we analyze if the performance of PretrainMD with two SSL tasks outperforms its isolated components, i.e. when using only one task for pre-training. The second ablation axis analyzes the benefit of the injection of noise for the generative SSL. As displayed in Table 2, the results clearly show that both SSL tasks contribute to the efficacy of learned representations. We further observe that the noise contributes significantly to the improvement of performance. Particularly, fine-tuning the pre-trained model with a noiseless generative task can lead to even worse predictions. This phenomenon supports our statement that noise can effectively increase the difficulty of pre-training task and prevent overfitting.

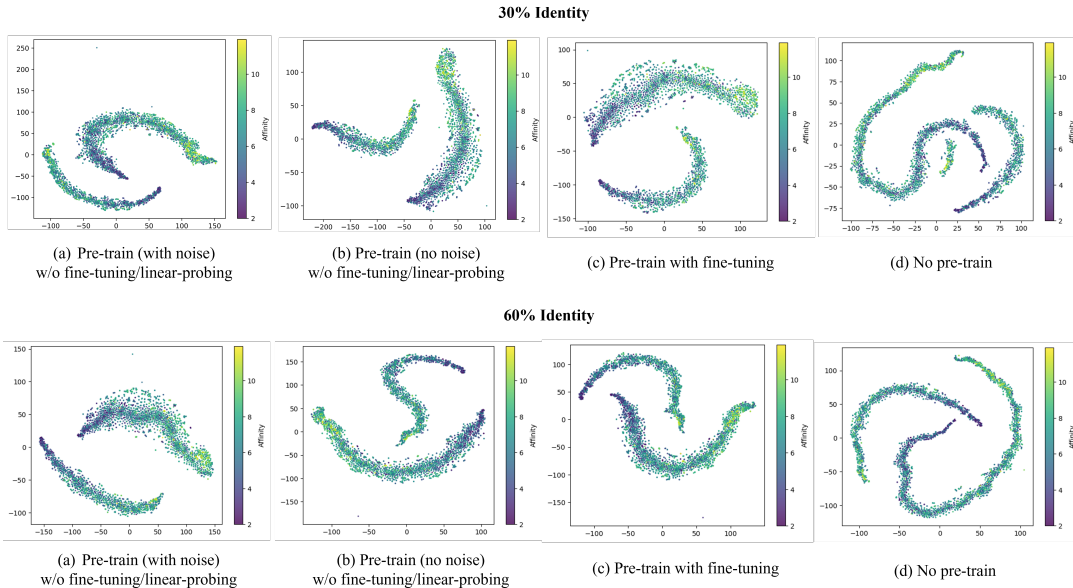


Figure 2: Dimensionality reduction of the protein-ligand representations using TSNE [60], color-coded based on the strength of corresponding binding affinities.

Table 2: **Ablation study on PretrainMD**, where DG and SO stand for the denoising generative task and the snapshot ordering task respectively. Results are documented for 3 runs.

	DG (Noise)	DG (No Noise)	SO	RMSD	R_p	R_s
No Pre-train	-	-	-	1.479 ± 0.030	0.564 ± 0.048	0.584 ± 0.041
Linear Probing	✓	-	-	1.419 ± 0.030	0.550 ± 0.047	0.568 ± 0.039
	-	✓	-	1.431 ± 0.028	0.536 ± 0.041	0.553 ± 0.035
	✓	-	✓	1.417 ± 0.021	0.548 ± 0.036	0.564 ± 0.042
Fine-tuning	✓	-	-	1.473 ± 0.034	0.564 ± 0.038	0.584 ± 0.039
	-	✓	-	1.543 ± 0.049	0.562 ± 0.044	0.580 ± 0.032
	✓	-	✓	1.461 ± 0.027	0.584 ± 0.045	0.602 ± 0.033

Moreover, as previously announced, even though our pre-training dataset only contains 64 protein-ligand pairs, our model realizes unexpected generalization to all 3K samples in PDBbind. Thus, we take a further step to investigate the influence of the number of pre-training samples over the performance in downstream tasks. As shown in Figure 3, when the number of proteins exceeds 50, the benefit for linear-probing is negligible. On the other hand, the improvement for fine-tuning persistently augments along with the increase of the number of pre-training samples.

5 Related Work

Protein-ligand modeling. With increasing availability of sequence and structure data, the area of protein representation learning has developed rapidly. Free energy-based simulations and machine learning-based scoring functions are two major computational methods for the binding affinity prediction [92], and the latter is data-driven and can fast screen a vast number of compounds, attaching increasing interests.

One-dimensional amino acid sequences continue to be the simplest and most abundant source of protein data, resulting in various methods [37, 16, 67] that borrow ideas from the area of NLP. Beyond that, previous methods ignore the spatial complexity of proteins and it has been proven that the exploitation of their 3D structures leads to improved performance [87, 3]. Some utilize 3D grids to capture the spatial distribution of the properties within molecular conformers, where 3DCNN [72, 40]

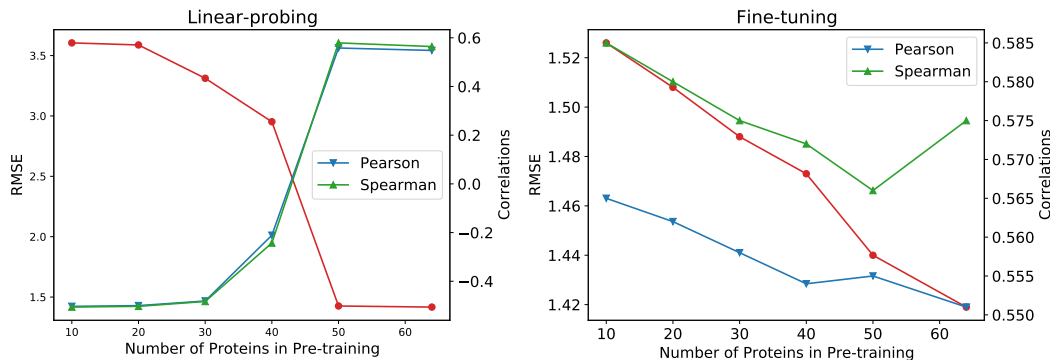


Figure 3: **Ablation study on the number of protein-ligand pairs used in the pre-training stage.** The left and right figures correspond to different strategies of linear-probing and fine-tuning.

have been the method of choice. Other studies use 3D voxel-based surface representations as inputs to 3DCNN [55, 66] for the prediction of protein-ligand binding sites [42]. However, none of those approaches consider a temporal perspective and take advantage of molecular dynamics simulations to describe the joint flexibility of proteins and ligands [36].

Protein self-supervised learning. Inspired by the progress in generative pre-training for language understanding [71], similar methods have been expanded to molecular property prediction [76, 97]. As for proteins, most preceding studies focus on pre-training on unlabeled amino acid sequences because of their abundance [6, 73, 24]. However, due to the fact that that protein functions are heavily governed by their folded structures, more and more attention has been draw to leverage the full spatial complexity of proteins. Hermosilla and Ropinski [34] uses contrastive learning for representation learning of 3D protein structures from the perspective of sub-structures. Apart from that, Zhang et al. [98] combines a multi-view contrastive learning and a self-prediction learning to encode geometric features of proteins. Then these semantic representations learned from SSL are utilized for downstream tasks including structure classification [35], model quality assessment [4], and function prediction [30]. Nevertheless, no preceding research excavate the potential of pre-training on this sort of spatial-temporal data, partly because of the high expenditure to run MD simulations.

6 Conclusion

Biological discovery demonstrates that the flexibility of both the receptor and ligand is deterministic in deciding the binding affinity, and MD simulations conventionally shoulder the responsibility to depict this dynamical process. In this work, in order to employ the time-dependent information inside MD trajectories, we introduce a simple yet effective pre-training paradigm from both spatial and temporal perspectives for protein representation learning called PretrainMD. It consists of two categories of self-supervised learning tasks: one is the atom-level denoising generative task and the other is the graph-level snapshot ordering task. We then linear probe and fine-tune the pre-trained models in the downstream drug binding prediction. Extensive experiments verify its effectiveness and ablation studies demonstrate the necessity of each component of our proposed PretrainMD.

References

- [1] Abagyan, R., Totrov, M., 2001. High-throughput docking for lead generation. *Current opinion in chemical biology* 5, 375–382.
- [2] An, G., 1996. The effects of adding noise during backpropagation training on a generalization performance. *Neural computation* 8, 643–674.
- [3] Atz, K., Grisoni, F., Schneider, G., 2021. Geometric deep learning on molecular representations. *Nature Machine Intelligence* , 1–10.
- [4] Baldassarre, F., Menéndez Hurtado, D., Elofsson, A., Azizpour, H., 2021. Graphqa: protein model quality assessment using graph convolutional networks. *Bioinformatics* 37, 360–366.
- [5] Ballester, P.J., Mitchell, J.B., 2010. A machine learning approach to predicting protein–ligand binding affinity with applications to molecular docking. *Bioinformatics* 26, 1169–1175.
- [6] Bepler, T., Berger, B., 2019. Learning protein sequence embeddings using information from structure. *arXiv preprint arXiv:1902.08661* .
- [7] Bepler, T., Berger, B., 2021. Learning the protein language: Evolution, structure, and function. *Cell systems* 12, 654–669.
- [8] Berman, H.M., Westbrook, J., Feng, Z., Gilliland, G., Bhat, T.N., Weissig, H., Shindyalov, I.N., Bourne, P.E., 2000. The protein data bank. *Nucleic acids research* 28, 235–242.
- [9] Berneche, S., Roux, B., 2001. Energetics of ion conduction through the k⁺ channel. *Nature* 414, 73–77.
- [10] Boehr, D.D., Nussinov, R., Wright, P.E., 2009. The role of dynamic conformational ensembles in biomolecular recognition. *Nature chemical biology* 5, 789–796.
- [11] Cai, C., Wang, Y., 2020. A note on over-smoothing for graph neural networks. *arXiv preprint arXiv:2006.13318* .
- [12] Changeux, J.P., Edelstein, S., 2011. Conformational selection or induced fit? 50 years of debate resolved. *F1000 biology reports* 3.
- [13] Chen, T., Kornblith, S., Norouzi, M., Hinton, G., 2020. A simple framework for contrastive learning of visual representations, in: *International conference on machine learning*, PMLR. pp. 1597–1607.
- [14] Chodera, J.D., Noé, F., 2014. Markov state models of biomolecular conformational dynamics. *Current opinion in structural biology* 25, 135–144.
- [15] Cui, B., Li, Y., Chen, M., Zhang, Z., 2018. Deep attentive sentence ordering network, in: *Proceedings of the 2018 Conference on Empirical Methods in Natural Language Processing*, pp. 4340–4349.
- [16] Dalkiran, A., Rifaioglu, A.S., Martin, M.J., Cetin-Atalay, R., Atalay, V., Doğan, T., 2018. Ecpred: a tool for the prediction of the enzymatic functions of protein sequences based on the ec nomenclature. *BMC bioinformatics* 19, 1–13.
- [17] De Vivo, M., Masetti, M., Bottegoni, G., Cavalli, A., 2016. Role of molecular dynamics and related methods in drug discovery. *Journal of medicinal chemistry* 59, 4035–4061.
- [18] Devlin, J., Chang, M.W., Lee, K., Toutanova, K., 2018. Bert: Pre-training of deep bidirectional transformers for language understanding. *arXiv preprint arXiv:1810.04805* .
- [19] Dror, R.O., Arlow, D.H., Maragakis, P., Mildorf, T.J., Pan, A.C., Xu, H., Borhani, D.W., Shaw, D.E., 2011a. Activation mechanism of the β 2-adrenergic receptor. *Proceedings of the National Academy of Sciences* 108, 18684–18689.
- [20] Dror, R.O., Green, H.F., Valant, C., Borhani, D.W., Valcourt, J.R., Pan, A.C., Arlow, D.H., Canals, M., Lane, J.R., Rahmani, R., et al., 2013. Structural basis for modulation of a g-protein-coupled receptor by allosteric drugs. *Nature* 503, 295–299.

- [21] Dror, R.O., Pan, A.C., Arlow, D.H., Borhani, D.W., Maragakis, P., Shan, Y., Xu, H., Shaw, D.E., 2011b. Pathway and mechanism of drug binding to g-protein-coupled receptors. *Proceedings of the National Academy of Sciences* 108, 13118–13123.
- [22] Durrant, J.D., McCammon, J.A., 2011. Molecular dynamics simulations and drug discovery. *BMC biology* 9, 1–9.
- [23] Eastman, P., Swails, J., Chodera, J.D., McGibbon, R.T., Zhao, Y., Beauchamp, K.A., Wang, L.P., Simmonett, A.C., Harrigan, M.P., Stern, C.D., et al., 2017. Openmm 7: Rapid development of high performance algorithms for molecular dynamics. *PLoS computational biology* 13, e1005659.
- [24] Elnaggar, A., Heinzinger, M., Dallago, C., Rihawi, G., Wang, Y., Jones, L., Gibbs, T., Feher, T., Angerer, C., Steinegger, M., et al., 2020. Prottrans: towards cracking the language of life's code through self-supervised deep learning and high performance computing. *arXiv preprint arXiv:2007.06225*.
- [25] Fischer, E., 1894. Einfluss der configuration auf die wirkung der enzyme. *Berichte der deutschen chemischen Gesellschaft* 27, 2985–2993.
- [26] Fischer, M., Coleman, R.G., Fraser, J.S., Shoichet, B.K., 2014. Incorporation of protein flexibility and conformational energy penalties in docking screens to improve ligand discovery. *Nature chemistry* 6, 575–583.
- [27] Frenkel, D., Smit, B., 2001. *Understanding molecular simulation: from algorithms to applications*. volume 1. Elsevier.
- [28] Gainza, P., Sverrisson, F., Monti, F., Rodola, E., Boscaini, D., Bronstein, M., Correia, B., 2020. Deciphering interaction fingerprints from protein molecular surfaces using geometric deep learning. *Nature Methods* 17, 184–192.
- [29] Ganesan, A., Coote, M.L., Barakat, K., 2017. Molecular dynamics-driven drug discovery: leaping forward with confidence. *Drug discovery today* 22, 249–269.
- [30] Gligorijević, V., Renfrew, P.D., Kosciolk, T., Leman, J.K., Berenberg, D., Vatanen, T., Chandler, C., Taylor, B.C., Fisk, I.M., Vlamakis, H., et al., 2021. Structure-based protein function prediction using graph convolutional networks. *Nature communications* 12, 1–14.
- [31] Godwin, J., Schaarschmidt, M., Gaunt, A.L., Sanchez-Gonzalez, A., Rubanova, Y., Veličković, P., Kirkpatrick, J., Battaglia, P., 2021. Simple gnn regularisation for 3d molecular property prediction and beyond, in: *International Conference on Learning Representations*.
- [32] Gong, J., Chen, X., Qiu, X., Huang, X., 2016. End-to-end neural sentence ordering using pointer network. *arXiv preprint arXiv:1611.04953*.
- [33] Han, J., Rong, Y., Xu, T., Huang, W., 2022. Geometrically equivariant graph neural networks: A survey. *arXiv preprint arXiv:2202.07230*.
- [34] Hermosilla, P., Ropinski, T., 2021. Contrastive representation learning for 3d protein structures.
- [35] Hermosilla, P., Schäfer, M., Lang, M., Fackelmann, G., Vázquez, P.P., Kozlíková, B., Krone, M., Ritschel, T., Ropinski, T., 2020. Intrinsic-extrinsic convolution and pooling for learning on 3d protein structures. *arXiv preprint arXiv:2007.06252*.
- [36] Hollingsworth, S.A., Dror, R.O., 2018. Molecular dynamics simulation for all. *Neuron* 99, 1129–1143.
- [37] Hou, J., Adhikari, B., Cheng, J., 2018. Deepsf: deep convolutional neural network for mapping protein sequences to folds. *Bioinformatics* 34, 1295–1303.
- [38] Hu, Z., Dong, Y., Wang, K., Chang, K.W., Sun, Y., 2020. Gpt-gnn: Generative pre-training of graph neural networks, in: *Proceedings of the 26th ACM SIGKDD International Conference on Knowledge Discovery & Data Mining*, pp. 1857–1867.

- [39] Jernite, Y., Bowman, S.R., Sontag, D., 2017. Discourse-based objectives for fast unsupervised sentence representation learning. *arXiv preprint arXiv:1705.00557* .
- [40] Jiménez, J., Skalic, M., Martinez-Rosell, G., De Fabritiis, G., 2018. K deep: protein–ligand absolute binding affinity prediction via 3d-convolutional neural networks. *Journal of chemical information and modeling* 58, 287–296.
- [41] Kahn, A.B., 1962. Topological sorting of large networks. *Communications of the ACM* 5, 558–562.
- [42] Kandel, J., Tayara, H., Chong, K.T., 2021. Puresnet: prediction of protein-ligand binding sites using deep residual neural network. *Journal of cheminformatics* 13, 1–14.
- [43] Kappel, K., Miao, Y., McCammon, J.A., 2015. Accelerated molecular dynamics simulations of ligand binding to a muscarinic g-protein-coupled receptor. *Quarterly reviews of biophysics* 48, 479–487.
- [44] Khafizov, K., Perez, C., Koshy, C., Quick, M., Fendler, K., Ziegler, C., Forrest, L.R., 2012. Investigation of the sodium-binding sites in the sodium-coupled betaine transporter betp. *Proceedings of the National Academy of Sciences* 109, E3035–E3044.
- [45] Kingma, D.P., Ba, J., 2014. Adam: A method for stochastic optimization. *arXiv preprint arXiv:1412.6980* .
- [46] Kingma, D.P., Dhariwal, P., 2018. Glow: Generative flow with invertible 1x1 convolutions. *Advances in neural information processing systems* 31.
- [47] Kingma, D.P., Welling, M., 2013. Auto-encoding variational bayes. *arXiv preprint arXiv:1312.6114* .
- [48] Köhler, J., Klein, L., Noé, F., 2019. Equivariant flows: sampling configurations for multi-body systems with symmetric energies. *arXiv preprint arXiv:1910.00753* .
- [49] Köhler, J., Klein, L., Noé, F., 2020. Equivariant flows: exact likelihood generative learning for symmetric densities, in: *International Conference on Machine Learning*, PMLR. pp. 5361–5370.
- [50] Larsson, G., Maire, M., Shakhnarovich, G., 2016. Learning representations for automatic colorization, in: *European conference on computer vision*, Springer. pp. 577–593.
- [51] Li, J., Shaikh, S.A., Enkavi, G., Wen, P.C., Huang, Z., Tajkhorshid, E., 2013. Transient formation of water-conducting states in membrane transporters. *Proceedings of the National Academy of Sciences* 110, 7696–7701.
- [52] Liang, R., Swanson, J.M., Madsen, J.J., Hong, M., DeGrado, W.F., Voth, G.A., 2016. Acid activation mechanism of the influenza a m2 proton channel. *Proceedings of the National Academy of Sciences* 113, E6955–E6964.
- [53] Lin, J., Nogueira, R., Yates, A., 2021. Pretrained transformers for text ranking: Bert and beyond. *Synthesis Lectures on Human Language Technologies* 14, 1–325.
- [54] Lindorff-Larsen, K., Piana, S., Dror, R.O., Shaw, D.E., 2011. How fast-folding proteins fold. *Science* 334, 517–520.
- [55] Liu, Q., Wang, P.S., Zhu, C., Gaines, B.B., Zhu, T., Bi, J., Song, M., 2021. Octsurf: Efficient hierarchical voxel-based molecular surface representation for protein-ligand affinity prediction. *Journal of Molecular Graphics and Modelling* 105, 107865.
- [56] Liu, Z., Li, Y., Han, L., Li, J., Liu, J., Zhao, Z., Nie, W., Liu, Y., Wang, R., 2015. Pdb-wide collection of binding data: current status of the pdbbind database. *Bioinformatics* 31, 405–412.
- [57] Logeswaran, L., Lee, H., 2018. An efficient framework for learning sentence representations. *arXiv preprint arXiv:1803.02893* .
- [58] Logeswaran, L., Lee, H., Radev, D., 2018. Sentence ordering and coherence modeling using recurrent neural networks, in: *Thirty-Second AAAI Conference on Artificial Intelligence*.

- [59] Ma, B., Shatsky, M., Wolfson, H.J., Nussinov, R., 2002. Multiple diverse ligands binding at a single protein site: a matter of pre-existing populations. *Protein science* 11, 184–197.
- [60] Van der Maaten, L., Hinton, G., 2008. Visualizing data using t-sne. *Journal of machine learning research* 9.
- [61] Malmstrom, R.D., Lee, C.T., Van Wart, A.T., Amaro, R.E., 2014. Application of molecular-dynamics based markov state models to functional proteins. *Journal of chemical theory and computation* 10, 2648–2657.
- [62] McCammon, J.A., Gelin, B.R., Karplus, M., 1977. Dynamics of folded proteins. *Nature* 267, 585–590.
- [63] Mesquita, D., Souza, A., Kaski, S., 2020. Rethinking pooling in graph neural networks. *Advances in Neural Information Processing Systems* 33, 2220–2231.
- [64] Miao, Y., Feher, V.A., McCammon, J.A., 2015. Gaussian accelerated molecular dynamics: unconstrained enhanced sampling and free energy calculation. *Journal of chemical theory and computation* 11, 3584–3595.
- [65] Miao, Y., McCammon, J.A., 2017. Gaussian accelerated molecular dynamics: Theory, implementation, and applications, in: *Annual reports in computational chemistry*. Elsevier. volume 13, pp. 231–278.
- [66] Mylonas, S.K., Axenopoulos, A., Daras, P., 2021. Deepsurf: a surface-based deep learning approach for the prediction of ligand binding sites on proteins. *Bioinformatics* 37, 1681–1690.
- [67] Öztürk, H., Özgür, A., Ozkirimli, E., 2018. Deepdta: deep drug–target binding affinity prediction. *Bioinformatics* 34, i821–i829.
- [68] Paszke, A., Gross, S., Massa, F., Lerer, A., Bradbury, J., Chanan, G., Killeen, T., Lin, Z., Gimelshein, N., Antiga, L., et al., 2019. Pytorch: An imperative style, high-performance deep learning library. *Advances in neural information processing systems* 32.
- [69] Perez, A., Morrone, J.A., Simmerling, C., Dill, K.A., 2016. Advances in free-energy-based simulations of protein folding and ligand binding. *Current opinion in structural biology* 36, 25–31.
- [70] Prabhumoye, S., Salakhutdinov, R., Black, A.W., 2020. Topological sort for sentence ordering. *arXiv preprint arXiv:2005.00432*.
- [71] Radford, A., Narasimhan, K., Salimans, T., Sutskever, I., 2018. Improving language understanding by generative pre-training.
- [72] Ragoza, M., Hochuli, J., Idrobo, E., Sunseri, J., Koes, D.R., 2017. Protein–ligand scoring with convolutional neural networks. *Journal of chemical information and modeling* 57, 942–957.
- [73] Rao, R., Bhattacharya, N., Thomas, N., Duan, Y., Chen, X., Canny, J., Abbeel, P., Song, Y.S., 2019. Evaluating protein transfer learning with tape. *Advances in neural information processing systems* 32, 9689.
- [74] Reymond, J.L., Awale, M., 2012. Exploring chemical space for drug discovery using the chemical universe database. *ACS chemical neuroscience* 3, 649–657.
- [75] Rives, A., Meier, J., Sercu, T., Goyal, S., Lin, Z., Liu, J., Guo, D., Ott, M., Zitnick, C.L., Ma, J., et al., 2021. Biological structure and function emerge from scaling unsupervised learning to 250 million protein sequences. *Proceedings of the National Academy of Sciences* 118.
- [76] Rong, Y., Bian, Y., Xu, T., Xie, W., Wei, Y., Huang, W., Huang, J., 2020. Self-supervised graph transformer on large-scale molecular data. *Advances in Neural Information Processing Systems* 33, 12559–12571.
- [77] Salmaso, V., Moro, S., 2018. Bridging molecular docking to molecular dynamics in exploring ligand-protein recognition process: an overview. *Frontiers in pharmacology* 9, 923.

- [78] Satorras, V.G., Hoogeboom, E., Welling, M., 2021. E (n) equivariant graph neural networks, in: International Conference on Machine Learning, PMLR. pp. 9323–9332.
- [79] Shan, Y., Kim, E.T., Eastwood, M.P., Dror, R.O., Seeliger, M.A., Shaw, D.E., 2011. How does a drug molecule find its target binding site? *Journal of the American Chemical Society* 133, 9181–9183.
- [80] Śledź, P., Caflisch, A., 2018. Protein structure-based drug design: from docking to molecular dynamics. *Current opinion in structural biology* 48, 93–102.
- [81] Somnath, V.R., Bunne, C., Krause, A., 2021. Multi-scale representation learning on proteins, in: Thirty-Fifth Conference on Neural Information Processing Systems.
- [82] Stärk, H., Ganea, O.E., Pattanaik, L., Barzilay, R., Jaakkola, T., 2022. Equibind: Geometric deep learning for drug binding structure prediction. *arXiv preprint arXiv:2202.05146*.
- [83] Sun, Y., Zheng, Y., Hao, C., Qiu, H., 2021. Nsp-bert: A prompt-based zero-shot learner through an original pre-training task–next sentence prediction. *arXiv preprint arXiv:2109.03564*.
- [84] Suomivuori, C.M., Gamiz-Hernandez, A.P., Sundholm, D., Kaila, V.R., 2017. Energetics and dynamics of a light-driven sodium-pumping rhodopsin. *Proceedings of the National Academy of Sciences* 114, 7043–7048.
- [85] Teague, S.J., 2003. Implications of protein flexibility for drug discovery. *Nature reviews Drug discovery* 2, 527–541.
- [86] Thomas, N., Smidt, T., Kearnes, S., Yang, L., Li, L., Kohlhoff, K., Riley, P., 2018. Tensor field networks: Rotation-and translation-equivariant neural networks for 3d point clouds. *arXiv preprint arXiv:1802.08219*.
- [87] Townshend, R.J., Vögele, M., Suriana, P., Derry, A., Powers, A., Laloudakis, Y., Balachandar, S., Jing, B., Anderson, B., Eismann, S., et al., 2020. Atom3d: Tasks on molecules in three dimensions. *arXiv preprint arXiv:2012.04035*.
- [88] Tuckerman, M., 2010. Statistical mechanics: theory and molecular simulation. Oxford university press.
- [89] Tuckerman, M.E., Martyna, G.J., 2000. Understanding modern molecular dynamics: Techniques and applications.
- [90] Vaswani, A., Shazeer, N., Parmar, N., Uszkoreit, J., Jones, L., Gomez, A.N., Kaiser, Ł., Polosukhin, I., 2017. Attention is all you need. *Advances in neural information processing systems* 30.
- [91] Vogt, A.D., Di Cera, E., 2012. Conformational selection or induced fit? a critical appraisal of the kinetic mechanism. *Biochemistry* 51, 5894–5902.
- [92] Wang, D.D., Zhu, M., Yan, H., 2021. Computationally predicting binding affinity in protein–ligand complexes: free energy-based simulations and machine learning-based scoring functions. *Briefings in Bioinformatics* 22, bbaa107.
- [93] Wang, R., Fang, X., Lu, Y., Wang, S., 2004. The pdbind database: Collection of binding affinities for protein- ligand complexes with known three-dimensional structures. *Journal of medicinal chemistry* 47, 2977–2980.
- [94] Wu, F., Bai, X., 2021. Insertgnn: Can graph neural networks outperform humans in toefl sentence insertion problem? *arXiv preprint arXiv:2103.15066*.
- [95] Wu, F., Zhang, Q., Radev, D., Cui, J., Zhang, W., Xing, H., Zhang, N., Chen, H., 2021. 3d-transformer: Molecular representation with transformer in 3d space. *arXiv preprint arXiv:2110.01191*.
- [96] Zhang, Q., Wang, Z., Han, Y., Yu, H., Jin, X., Chen, H., 2022a. Prompt-guided injection of conformation to pre-trained protein model. *arXiv preprint arXiv:2202.02944*.

- [97] Zhang, Z., Liu, Q., Wang, H., Lu, C., Lee, C.K., 2021. Motif-based graph self-supervised learning for molecular property prediction. *Advances in Neural Information Processing Systems* 34.
- [98] Zhang, Z., Xu, M., Jambas, A., Chenthamarakshan, V., Lozano, A., Das, P., Tang, J., 2022b. Protein representation learning by geometric structure pretraining. *arXiv preprint arXiv:2203.06125* .

A Equivariant Graph Neural Network

We utilize the EGNN [78] as our base protein encoder. To begin with, we represent the protein-ligand pairs as spatial k-nearest neighbor (KNN) graphs. Each atom is connected in the graph to the closest 32 other nodes. Then the layer of EGNN is formally defined as the following:

$$\mathbf{m}_{ij} = \phi_e \left(\mathbf{h}_i^{(t),l}, \mathbf{h}_j^{(t),l}, \left\| \mathbf{x}_i^{(t),l} - \mathbf{x}_j^{(t),l} \right\|^2 \right), \quad (3)$$

$$\mathbf{x}_i^{(t),l+1} = \mathbf{x}_i^{(t),l} + C \sum_{j \neq i} \left(\mathbf{x}_i^{(t),l} - \mathbf{x}_j^{(t),l} \right) \phi_x(\mathbf{m}_{ij}), \quad (4)$$

$$\mathbf{m}_i = \sum_{j \neq i} \mathbf{m}_{ij}, \quad (5)$$

$$\mathbf{h}_i^{(t),l+1} = \phi_h \left(\mathbf{h}_i^{(t),l}, \mathbf{m}_i \right), \quad (6)$$

where ϕ_e is the edge operation, and ϕ_h denotes the node operation that aggregates the messages \mathbf{m}_i and the node embeddings $\mathbf{h}_i^{(t),l}$ to acquire the updated node embedding $\mathbf{h}_i^{(t),l+1}$. ϕ_x takes as input the edge embedding \mathbf{m}_{ij} as the weight to sum all relative distance $\mathbf{x}_i^{(t),l} - \mathbf{x}_j^{(t),l}$ and output the renewed coordinates $\mathbf{x}_i^{(t),l+1}$.

B Experimental Setup

B.1 Molecular dynamics simulations

It takes a V100 GPU approximately 22 hours to run 100 nanosecond (ns) for each protein-ligand pair in the water-solvent environment. To simulate all 64 pairs, we spend xxx hours on xxx GPUs.

B.2 Experimental details

EGNN architecture. We use a 3-layer EGNN with a hidden dimensionality of 32. We adopt the coordinate normalization and a sum pooling method. The coordinate clamping value is set as 2. No dropout is used for any layer. The maximum number of nodes for the input graph is set as 10000.

Dataset splits. According to Townshend et al. [87], the split based on a 30% sequence identity threshold leads to training, validation, and test sets of size 3507, 466, and 490, respectively. The split based on a 60% sequence identity threshold leads to training, validation, and test sets of size 3678, 460, and 460, respectively.

B.3 Training details.

We use Pytorch [68] to implement EGNN and a random seed of 1234. On the pre-training stage, utilize the distributed training with 4 V100 GPUs and a batch size of 32 for each GPU. An Adam [45] optimizer is used and a ReduceLROnPlateau scheduler is enforced to adjust it with a factor of 0.6 and a patience of 10. The initial learning rate is 1e-4, and we apply no weight decay there. Each model is trained with 200 epochs. We split the trajectory of each protein-ligand pair into training and validation with a ratio of 9:1, and save the best model based on its performance on the validation set.

On the downstream fine-tuning stage, the number of GPUs, the configurations of optimizer and scheduler keep the same. The batch size is 64. Following Townshend et al. [87], we also only use the pocket position and the ligand as the model input. Only atoms within a distance of 6 Å from the ligand are used and the number of atoms in total (ligand + protein) is limited to no more than 600. We perform a hyperparameter sweep in Table 3 for different pre-training models and different strategies of linear-probing and fine-tuning.

B.4 Baselines

For protein-ligand binding affinity prediction, we use the reported values from Somnath et al. [81] and Townshend et al. [87]. As for the model size, we use all available reported numbers from Somnath

Table 3: The training hyper-parameters.

Hyper-parameter	Description	Range
lr	The initial learning rate of ReduceLROnPlateau learning rate scheduler.	$[1e-4, 1e-5]$
min_lr	The minimum learning rate of ReduceLROnPlateau learning rate scheduler.	$[5e-6, 5e-7]$

et al. [81]. For 3DCNN and 3DGCN [87], we download the code from the official repository ² and compute the model parameters.

B.5 Visualization details.

For the visualization in the main text, we apply the same setting of the t-SNE algorithm to the presentations of protein-ligand pairs \mathbf{H} for the dimension reduction. Concretely, the maximal iteration is 10000. The perplexity is 30.0. The learning rate is 200. The early exaggeration is 12.0. The angle is 0.5. Finally, the t-SNE reduces the outputs of EGNN into the 2-dimensional representations, which then are plotted as 2D images.

²3DCNN: <https://github.com/drordlab/atom3d/blob/master/examples/lba/cnn3d/train.py#L179>; 3DGCN: <https://github.com/drordlab/atom3d/blob/master/examples/lba/gnn/train.py>